

[V]

研究成果の刊行物・別刷

症例報告

完全型 pachydermoperiostosis の 1 例

種瀬 啓士 若林亜希子 山本 晃三 宮川 俊一
今西 智之

臨床皮膚科

第64巻 第3号 別刷

2010年3月1日 発行

医学書院

完全型 pachydermoperiostosis の 1 例*

種瀬 啓士*¹・若林亜希子*¹・山本 晃三*¹
宮川 俊一*¹・今西 智之*²

要 約 41 歳，男性。17 歳時に頭部の皮膚が肥厚していることを自覚した。加齢とともに徐々に顕著となり，皺襞を形成するようになった。初診時頭部は脳回転状皮膚を，指趾末節は太鼓ばち状を呈し，X 線では橈骨・尺骨に骨膜性骨肥厚があり，本症例を完全型 pachydermoperiostosis と診断した。本疾患は，太鼓ばち状指趾，皮膚の肥厚性変化・脳回転状皮膚，四肢遠位骨の骨膜性骨肥厚を主徴とする皮膚形成異常症である。近年，本疾患家系において HPGD 遺伝子が原因遺伝子として同定され，その病態が明らかになりつつある。

キーワード pachydermoperiostosis, 15-ヒドロキシプロスタグランジン脱水素酵素, HPGD 遺伝子

種瀬啓士，他：臨皮 64：221-224，2010

はじめに

Pachydermoperiostosis(以下，PDP)は，太鼓ばち状指趾，皮膚の肥厚性変化・脳回転状皮膚，四肢遠位骨の骨膜性骨肥厚を主徴とする，皮膚形成異常症である¹⁾。1868 年に Friedrich²⁾によって記載されて以降，厚皮骨膜症，Touraine-Solente-Golé 症候群，肥大性皮膚骨膜症，特発性肥厚性皮膚骨膜症などの病名で報告され，本邦においても Ota³⁾の報告以降 100 例を超える報告がなされている^{4,5)}。その徴候の出現頻度，程度は症例により異なる¹⁾。今回われわれは，3 主徴を認め，完全型 PDP と診断した症例を経験したので，若干の文献的な考察を加えて報告する。

症 例

患 者：41 歳，男性

主 訴：頭皮の肥厚および深い皺襞

初 診：2008 年 6 月

家族歴：特記すべきことなし。

既往歴：精神発達遅滞

現病歴：17 歳頃に頭部皮膚肥厚を自覚した。以後顕著となったため，精査目的にて当院脳外科および皮膚科を受診した。

現 症：身長 188 cm，体重 88.5 kg，上肢長 85 cm，下肢長 90 cm，足長 29 cm。前額部および被髪頭部の皮膚が全体に肥厚し皺襞を形成し，いわゆる脳回転状皮膚を呈していた(図 1 a，

* A case of the complete form of pachydermoperiostosis

¹ Keiji TANESE, Akiko WAKABAYASHI, Kozo YAMAMOTO and Shunichi MIYAKAWA : 川崎市立川崎病院(主任：宮川 俊一部長) Division of Dermatology, Kawasaki Municipal Hospital, Kanagawa, Japan (Chief : Dr S MIYAKAWA)

² Nobuyuki IMANISHI : 川崎市立川崎病院脳神経外科(主任：今西 智之部長) Division of Brain Surgery, Kawasaki Municipal Hospital, Kanagawa, Japan (Chief : Dr T IMANISHI)
〔論文責任者〕種瀬 啓士：川崎市立川崎病院皮膚科(☎ 210-0013 川崎市川崎区新川通 12-1)

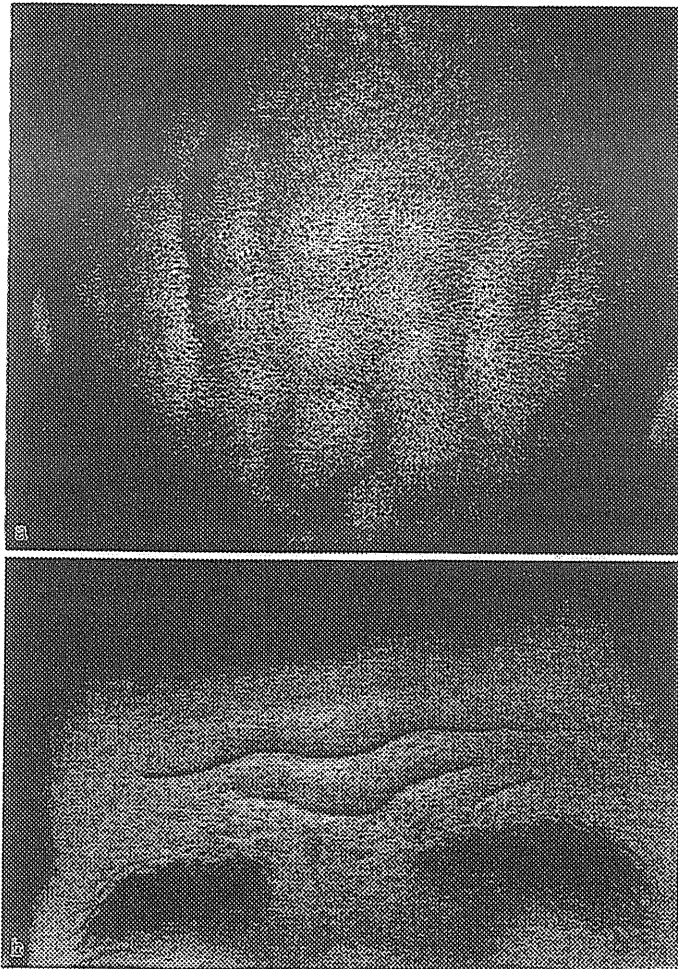


図1 臨床像

a：頭部の皮膚は肥厚し皺襞を形成，いわゆる脳回転状皮膚を呈する。

b：前額部の皮膚にも同様の肥厚，皺襞に加えて皮脂分泌亢進による油状光沢を認める。

b). 顔面の皮膚は皮脂分泌亢進による油状光沢を認めた。指趾末節は腫大し太鼓ばち状に，爪甲は時計皿状であった(図2)。全身症状は，発毛障害・性器発育障害を含め認めなかった。

臨床検査所見：尿・血液一般検査，生化学検査では異常はなかった。内分泌検査においても，成長ホルモン，甲状腺ホルモン，性ホルモンを含む各種血中ホルモン濃度に異常はなかった。心電図，胸部X線では正常で，頭部MRIにおいてもトルコ鞍の拡大はなく，下垂体腺腫も認めなかった。前腕の骨単純X線では，橈骨・尺骨ともに骨膜性骨肥厚がみられ，全体的に棒状を呈していた(図3)。

病理組織学的所見：頭部の隆起した皮膚より生検を施行した。真皮は全体に肥厚し，脂腺の増加

が認められた。膠原線維は肥厚し，線維束間は浮腫性に変化していた(図4a)。膠原線維間および血管周囲性にリンパ球が軽度に浸潤していた。真皮内の浮腫性変化を呈する部位はアルシアン・ブルー染色pH2.5(図4b)，およびコロイド鉄染色にて陽性で，PAS染色陰性でヒアルロン酸を含む基質が沈着していることが示唆された。以上の所見より，本症例を完全型PDPと診断した。

要約

考 按

PDPの3主徴の出現頻度および程度は症例により異なり，Touraineらは主症状をもとに本症を以下の3型に分類している¹⁾。

(1) 完全型：皮膚の肥厚性変化，太鼓ばち状指趾および骨膜性骨新生の主症状をすべて備えた

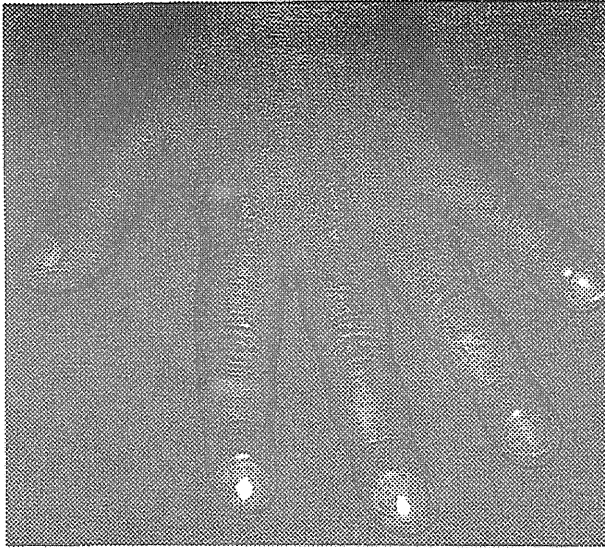


図2 臨床像
手指末節の腫大，太鼓ばち状指，時計皿状爪甲を認める。

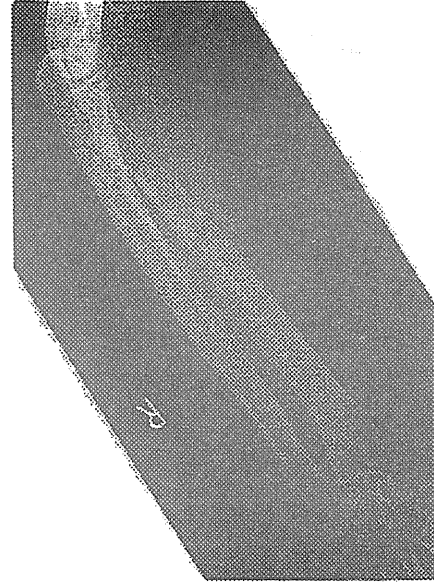


図3 X線像
橈骨・尺骨に骨膜性骨肥厚がみられ，全体的に棒状を呈する。

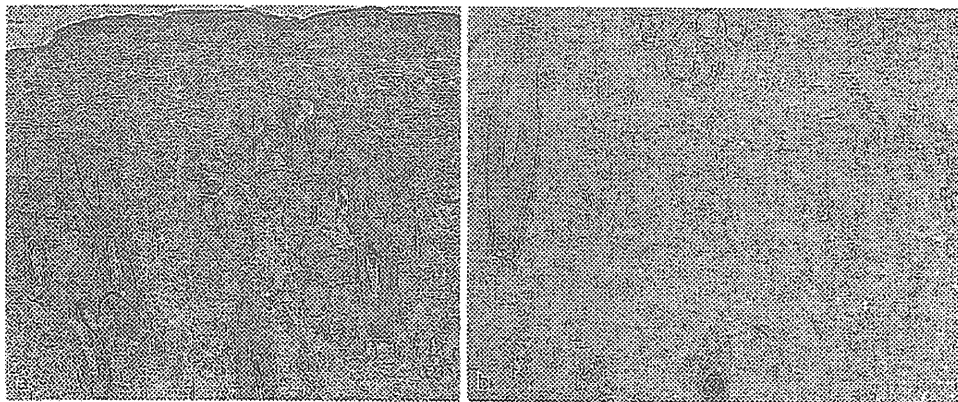


図4 病理組織学的所見
a: HE染色像。真皮は全体に肥厚し，脂腺の増加が認められる。膠原線維は肥厚し，線維束間は浮腫性に変化している。
b: アルシアン・ブルー染色(pH 2.5)。真皮内の青染像

もの。

(2) 不完全型：皮膚の肥厚性変化を欠くもの。

(3) 初期型：骨変化が軽度，または欠如し，皮膚肥厚のみを認めるもの。

Matucci-Cerinicら⁶⁾は，3主徴のほかに脂漏，多汗，毛囊炎，関節痛，指趾骨融解症，胃炎もしくは胃潰瘍，胃皺襞の肥厚，交感神経機能亢進を副症状として挙げている。

増田ら⁴⁾による131例の本邦報告の検討によれば，多くの症例は思春期に発症し(平均17歳)，10数年進行した後に症状が安定する。加齢とともに特徴的な症状が揃うため，自験例と同様に本症と診断されるまでに時間を要することが多い。男女比は圧倒的に男性に多い(15:1)。自験例では認めなかったものの，家族内発症は27%にみられる。遺伝形式は伴性劣性，常染色体優性遺

伝, 常染色体劣性遺伝など, さまざまな報告がある⁴⁾.

鑑別診断として, 肺気腫や気管支癌などの呼吸器系疾患に伴う肺性肥厚性骨関節症, 甲状腺疾患に伴う甲状腺性先端症およびチアノーゼ性心疾患に続発する二次性肥厚性骨関節症と末端肥大症がある⁴⁾. これらの疾患はしばしば本症と同様の臨床症状を呈するため, 確定診断のためには自験例と同様に全身検索を施行のうえ, 内分泌異常および肺・心疾患の存在を否定する必要がある.

肥厚した皮膚の病理組織像は脂腺・汗腺の増加, 膠原線維の肥厚および酸性ムコ多糖の沈着, リンパ球浸潤であり⁴⁾, 自験例においても同様の所見が得られた. この機序として, Wegrowskiらは病変部線維芽細胞の蛋白・コラーゲン合成低下と, ムコ多糖産生亢進を指摘している⁷⁾.

本疾患の病因について, Uppalら⁸⁾は本疾患患者を有する4家系を同祖接合体マッピング法により解析した. その結果, 4番染色体のq33-q34領域にある15-ヒドロキシプロスタグランジン脱水素酵素をコードする*HPGD*遺伝子を原因遺伝子として同定した. 15-ヒドロキシプロスタグランジン脱水素酵素はプロスタグランジン(以下, PG)分解酵素の1つである.*HPGD*遺伝子の変異がホモ接合性の患者は, PGE₂の慢性的な上昇に伴いPDPを発症し, 変異がヘテロ接合性の血縁者もより軽度な生化学的および臨床的な徴候を示す⁹⁾.

皮膚組織へのPGの蓄積が本疾患の症状形成にどのようにかかわっているかは今後の検討課題と

いえる. PGとムコ多糖産生亢進との関連性については, 耳鼻科領域においては声帯由来線維芽細胞においてPGE₂がヒアルロン酸合成酵素-1, 2の活性を亢進させ, ヒアルロン酸合成が促進されるとの報告がある⁹⁾. しかし, PG蓄積と骨膜性骨肥厚の関係については検討がなされていない. また, 完全型および不完全型の違いや本症が圧倒的に男性に多い理由を*HPGD*遺伝子の異常とPGの蓄積のみで説明すること困難である.

本疾患は遺伝性疾患としての報告のみならず, 内分泌障害^{10,11)}, 自律神経異常¹²⁾としての報告もある. したがって, PGの蓄積以外の要因が本疾患の発症にかかわっていることも想定され, さらなる症例の蓄積および病態の解明が望まれる.

本論文の要旨は第72回日本皮膚科学会東京支部学術大会において報告した.

文 献

- 1) Touraine A, et al: Presse Med 43: 1820, 1935
- 2) Friedreich N: Arch Path Anat 43: 83, 1868
- 3) Ota M: Dermatol Wochenschr 92: 345, 1935
- 4) 増田邦男, 他: 臨皮 54: 400, 2000
- 5) 松田やよい, 他: 臨と研 85: 1475, 2008
- 6) Matucci-Cerinic M, et al: Ann Rheum Dis 48: 240, 1989
- 7) Wegrowski Y, et al: J Invest Dermatol 106: 70, 1996
- 8) Uppal S, et al: Nat Genet 40: 789, 2008
- 9) Lim X, et al: Ann Otol Rhinol Laryngol 117: 227, 2008
- 10) Bianchi L, et al: Br J Dermatol 132: 128, 1995
- 11) 嶋田達也, 他: 内科 52: 191, 1983
- 12) Huckstep RL, Bodkin PE: Lancet 2: 343, 958

MEDICAL BOOK INFORMATION

医学書院

医療経済学で読み解く医療のモンダイ

真野俊樹

●A5 頁232 2008年
定価2,625円(本体2,500円+税5%)
[ISBN978-4-260-00659-0]

医療経済学の視点から医療の制度・仕組みを考察するユニークな“医療入門”。日本の医療費は高い? 今後病院数は増える? 減る? 後発薬の普及はなぜ進まない? DPCは医療費抑制に有効? 在院日数が減れば医療費も減る? 等々、気になる論点を経済学者であり医師でもある著者がわかりやすく解説する。医療経済学のエッセンスに触れつつ、日本の医療の現状・問題点を把握することができる。

症例報告

肥厚性皮膚骨膜炎の1例

重松由紀子 新関 寛徳 野崎 誠 佐々木りか子
堀川 玲子 関 敦仁 中川 温子 土居 博美
椛島 健治

臨床皮膚科

第64巻 第10号 別刷

2010年9月1日 発行

医学書院

肥厚性皮膚骨膜炎の1例*

重松由紀子*¹・新関 寛徳*¹・野崎 誠*¹
 佐々木りか子*^{1,2}・堀川 玲子*³・関 敦仁*⁴
 中川 温子*⁵・土居 博美*⁶・椛島 健治*⁶

要 約 19歳，男性，既往歴，家族歴に特記することはない。13歳頃より手指末端肥大が出現した。ばち指を認めたが，内分泌系・呼吸器・循環器系の疾患の異常はみられなかった。四肢の骨 X線像では，長管骨骨幹部骨皮質が肥厚していた。頭部に脳回転状皮膚は明らかではなかった。前額部左側皮膚生検で膠原線維の増生と脂腺の過形成，および汗腺の増加がみられた。本症の3主徴であるばち指，骨膜性骨肥厚，皮膚肥厚性変化を認めたが，頭部脳回転状皮膚がなかったため，不全型肥厚性皮膚骨膜炎と診断した。本症は，疾患特異的検査が存在せず，加齢とともに特徴的な症状が揃うため，時に診断に苦慮する。近年，原因遺伝子の検索がきっかけとなり，血中・尿中プロスタグランジン(PG)E₂濃度が高い症例が報告されたが自験例では正常範囲であった。今後 PGE₂を含む生理活性物質の検索が，診断や臨床病型分類に活用されよう。

キーワード 肥厚性皮膚骨膜炎，肥大性骨関節症，ばち指，骨膜性骨肥厚，脳回転様皮膚

重松由紀子，他：臨皮 64：751-754，2010

はじめに

肥厚性皮膚骨膜炎(pachydermoperiostosis：PDP)は，太鼓ばち状指(ばち指)，長管骨を主とする骨膜性骨肥厚，皮膚肥厚性変化(頭部脳回転状皮膚を含む)を3主徴とする疾患である。本疾患は，1868年，Friedreich¹⁾が，3主徴を有する症例を最初に記載した後，種々の名称で報告されてきた。1935年，Touraineら²⁾によって本症の

概念が明らかにされ，Touraine-Solente-Gole症候群と呼ばれるようになった。現在では，Vague³⁾の提唱したpachydermoperiostosisの名称が一般によく用いられている。

Touraineら²⁾は，その臨床所見より3型に分類している。すなわち，3主徴すべてを有する完全型(complete form)，頭部脳回転状皮膚を欠く不全型(incomplete form)，骨変化が軽度または

* A case of pachydermoperiostosis

^{*1} Yukiko SHIGEMATSU, Hironori NIIZEKI, Makoto NOZAKI and Rikako SASAKI：国立成育医療研究センター皮膚科 Department of Dermatology, National Center for Child Health and Development, Tokyo, Japan

^{*2} Rikako SASAKI：りかこ皮膚科クリニック Rikako Dermatology Clinic, Tokyo, Japan

^{*3} Reiko HORIKAWA：国立成育医療研究センター内分泌代謝科 Department of Endocrinology and Metabolism, National Center for Child Health and Development, Tokyo, Japan

^{*4} Atsuhito SEKI：国立成育医療研究センター整形外科 Department of Orthopedics, National Center for Child Health and Development, Tokyo, Japan

^{*5} Atsuko NAKAGAWA：国立成育医療研究センター病理診断科 Department of Pathology, National Center for Child Health and Development, Tokyo, Japan

^{*6} Hiromi DOI and Kenji KABASHIMA：京都大学大学院医学研究科皮膚生命科学講座 Department of Dermatology, Kyoto University Graduate School of Medicine, Kyoto, Japan
 (論文責任者) 重松由紀子：国立成育医療研究センター皮膚科(☎ 157-8535 東京都世田谷区大蔵 2-10-1)

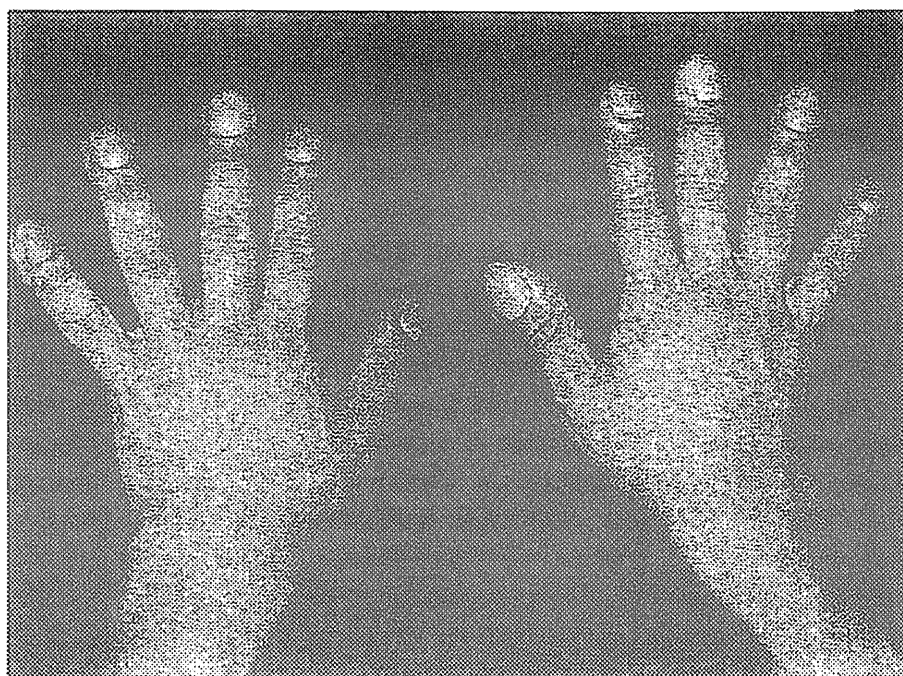


図1 臨床像(手指)
手指末端は肥大して太鼓ばち状を呈し、爪甲も肥大・彎曲して時計皿様である。

欠如する初期型 (forme fruste) である。今回われわれは、脳回転状皮膚を欠く不全型の症例を経験したので報告する。

症例

症例

患者：19歳，男性，職業，自動車整備士

主訴：手指末端肥大

家族歴：両親，同胞に同症を認めない。

既往歴：特記すべきことなし。

現病歴：13歳頃より手指末端肥大を自覚したが，医療機関には出向かずに放置していた。17歳時にたまたま外傷にて受診した整形外科医よりばち指を指摘された。内科にて心エコー，肺機能検査を行ったが，特記すべき異常所見はみられなかった。19歳時に経過観察のため同医を受診し，精査加療目的に当院内内分泌・代謝科を紹介され，皮膚症状につき当科を受診した。

現症：身長165.8cm，体重51.7kg。顔面・頭部の皮膚肥厚は明らかではなく，いわゆる獅子様顔貌や前額・被髪部に脳回転状皮膚は認められなかった。前額部に油性光沢があった。手指

末端は肥大してばち指となり，爪甲も肥大・彎曲して時計皿状となっていた(図1)。足趾についても同様であった。手掌に多汗症があった。

臨床検査成績：尿・血液一般検査，生化学検査，電解質は正常範囲内であった。末端肥大症の鑑別目的で行ったブドウ糖負荷試験では成長ホルモンの有意な抑制を認め，プロモクリプチン負荷試験では成長ホルモンの有意な抑制は認めなかった(いずれも正常反応を示した)。一方，TRH負荷試験では，通常TRHに対し分泌反応を示さない成長ホルモンの分泌反応を認めた。これは末端肥大症で認められる反応ではあるが，思春期には正常でも認められ(奇異反応)，後者によるものと診断した。頭部MRIでは下垂体を含めて脳実質に特記すべき異常はなかった。以上より，ばち指を生じる疾患として，内分泌学的異常による末端肥大症は否定的であり，PDPを疑った。心電図，胸部X線検査を行い呼吸器・循環器系疾患の検索を行ったが，正常であった。四肢の骨単純X線像では，長管骨骨幹部の骨皮質が肥厚していた(図2a)。手指において，中手骨・基節骨の骨幹

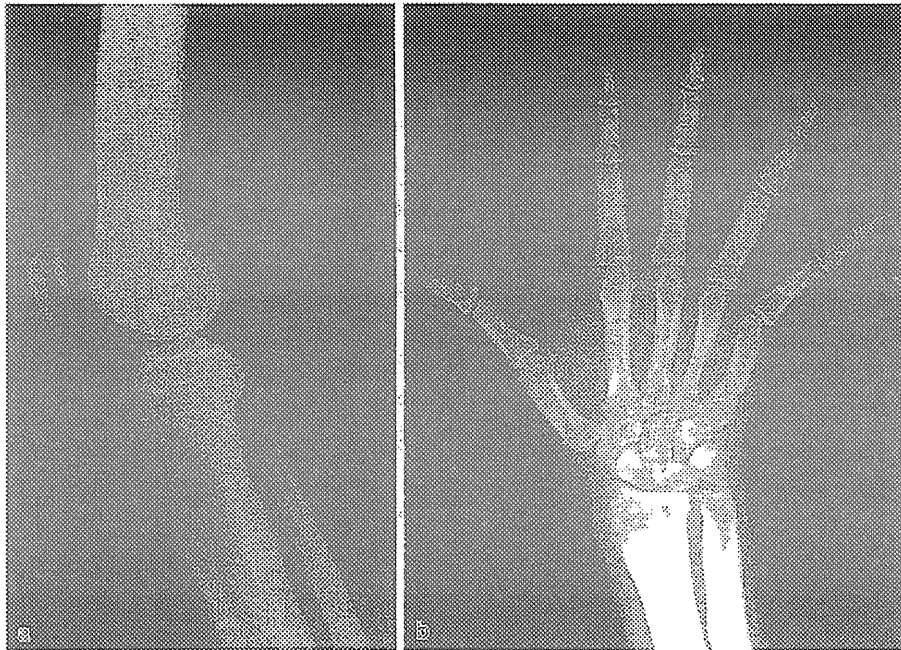


図2 単純X線像

- a：右膝関節，四肢の長管骨骨幹部骨皮質の肥厚を認める。
 b：右手，手指では，中手骨・基節骨の骨幹部骨皮質の肥厚がみられる。



図3 病理組織像(左前額部，HE染色)
 真皮内に膠原線維の増生と脂腺の過形成，および汗腺の増加を認める。

部骨皮質が肥厚していた(図2b)。

病理組織学的所見：左前額部の皮膚より生検した。表皮に著変はなかったが，真皮では，肥大した膠原線維と脂腺の過形成，および汗腺の増加が認められた。膠原線維は，皮下脂肪織へも進展し，付属器の上昇がみられた。以上より，真皮が



図4 病理組織像(左前額部，アルシアンブルー染色)
 膠原線維は肥大し，線維束間には青染する物質の沈着がみられる。

肥厚していると考えた(図3)。増生した膠原線束間には，酸性ムコ多糖と考えられるアルシアンブルー陽性物質が沈着していた(図4)。

血中 PGE₂ 濃度測定：静脈血を採取後(血清分離し)，ただちに-80°C保存した。各サンプルは測定時 20 倍希釈し，PGE₂ (プロスタグランジン E₂) 測定 ELISA キットにより測定した(Prostaglandin E₂ Kit-Monoclonal, Cayman Chemical,

USA：京都大学大学院医学研究科皮膚生命科学講座において測定）。患者血清 PGE₂ 値は 30 pg/ml であった（健常家族の血清では 29.5 pg/ml）。概ね 1,000 pg/ml 以上が異常値であるので、正常範囲であった。

診断および経過：自験例は、PDP の 3 主徴のうち、ばち指、長管骨を主とする骨膜性骨肥厚、皮膚肥厚性変化を認めた。しかし、発症後約 10 年を経た 2010 年 2 月現在でも、前額部・頭部にははっきりとした脳回転状皮膚を観察しえなかったため、不全型 PDP と診断した。PDP の合併症である顔面・胸背部の瘡瘻に対し、アダパレンを外用しているが、再発・寛解を繰り返している。



考 按

自験例は、PDP において合併が知られている貧血などはみられず、家族内発症もなく、いわゆる 3 徴のみで診断した。関節症状のみられる PDP は原発性肥大性骨関節症 (primary hyperostrophic osteoarthropathy : PHO) とほぼ同義であり、二次性 (主に肺性) 肥大性骨関節症との鑑別が問題になる。自験例では、内分泌学的異常を伴わず末端肥大症が否定された。また、呼吸器疾患などの基礎疾患も見いだされず、発症が十代であることより、原発性 (遺伝性) PDP と診断した。このように PDP は従来、疾患特異的検査が存在しなかったため、時に診断に苦慮する症例があると考えられる。しかし、2008 年に原因遺伝子が同定され、新たな展開がみられた。

Uppal⁴⁾ は、パキスタン人 PHO 家系から NAD (+)-dependent 15-hydroxyprostaglandin dehydrogenase (HPGD) 遺伝子に変異を見いだした。HPGD 遺伝子は PGE₂ の分解酵素をコードしており、その欠損により患者血中の過剰に残存した PGE₂ が尿中に排泄されることも報告された。Uppal⁴⁾ が報告した症例は、いずれも骨病変が顕著な症例であり、Touraine²⁾ の提唱した 3 型のうち、いずれが HPGD 遺伝子の変異により生じる病型なのか、あるいは 3 つの病型は、

同一遺伝子内の変異の位置と関連したものなのか (genotype-phenotype correlation) はいまだ明らかになっていない。

Kabashima⁵⁾ は、完全型 2 例において HPGD 遺伝子変異の検索および血中 PGE₂ 濃度測定を行い、変異は発見されず、PGE₂ 濃度も上昇していなかったことを報告している。彼らの検索した 2 例はいずれも皮膚肥厚の強い完全型の症例であったことから、HPGD 遺伝子は不全型の一部の症例の原因遺伝子であり、PDP の成因には複数の原因遺伝子が存在すると考察している。自験例においては、皮膚肥厚はあまり強くないが、はっきりとしたばち指と骨膜肥厚があり、不全型と考えられる。しかし、HPGD 遺伝子変異例で観察される関節症状はみられず、前述の PHO という診断には合致しない。今後、関節症状や頭部脳回転状皮膚の出現があれば、病型の再検討をすべきであるが、現在のところ不全型と診断せざるを得ない症例と考えられる。なお、過去 21 年間 (1989 年以降) の本邦原著論文を検討したが、病型が観察期間中 (初診以後) 変化したと考えられる症例はみられなかった。完全型、不全型の報告年齢に有意差がなかったため、病型の移行は通常はみられないと推測している。

当該疾患では血中 PGE₂ 濃度は異常値を示さなかったが、今後血中・尿中 PGE₂ 濃度が病型に関連しているかどうかを検討するためにさらなる症例の集積が待たれる。

本論文の一部は厚生労働科学研究費補助金 (難治性疾患克服研究事業) による助成を受けた。

本論文の要旨は日本皮膚科学会第 826 回東京地方会 (2009 年 9 月) において発表した。

文 献

- 1) Friedreich N: Virchows Arch [a] 43: 83, 1986
- 2) Touraine A, et al: Presse Med 43: 1820, 1935
- 3) Vague J: Ann Med 51: 152, 1950
- 4) Uppal S, et al: Nat Genet 40: 789, 2008
- 5) Kabashima K, et al: Am J Pathol 176: 721, 2010

Epithelial and Mesenchymal Cell Biology

Involvement of Wnt Signaling in Dermal Fibroblasts

Kenji Kabashima,^{*†‡} Jun-ichi Sakabe,^{*}
Ryutaro Yoshiki,^{*} Yasuhiko Tabata,[§]
Kimitoshi Kohno,[¶] and Yoshiki Tokura^{*}

From the Departments of Dermatology^{*} and Molecular Biology,[¶] School of Medicine, University of Occupational and Environmental Health, Kitakyushu; the Department of Dermatology,[†] and Center for Innovation in Immunoregulative Technology and Therapeutics,[‡] Kyoto University Graduate School of Medicine, Kyoto; and the Institute for Frontier Medical Sciences,[§] Kyoto University, Kyoto, Japan

Pachydermoperiostosis (PDP) is a rare disease characterized by unique phenotypes of the skin and bone, such as thick skin, implying that it may be caused by dysregulation of mesenchymal cells. The aim of this study is to examine the roles of dermal fibroblasts in the pathogenesis of pachydermia in association with Wnt signaling. The numbers of cultured fibroblasts were compared between healthy donors and PDP patients, and mRNA expression profiles in cultured dermal fibroblasts were examined by DNA microarray analysis and real-time reverse transcription-PCR. DKK1 and β -catenin protein expressions were also evaluated by immunohistochemistry in the skin. To evaluate the *in vivo* roles of DKK1 in mice, *DKK1* small interfering RNA was injected to the ears. We found that PDP fibroblasts proliferated more than control fibroblasts and that mRNA expression of a Wnt signaling antagonist, *DKK1*, was much lower in PDP fibroblasts than in normal ones. Consistently, decreased expression of DKK1 in fibroblasts and enhanced expression of β -catenin were noted in PDP patients. Moreover, recombinant human DKK1 protein decreased the proliferation of dermal fibroblasts. In accord with the above human studies, intradermal injections of *DKK1* small interfering RNA into mouse ears increased ear thickness as seen in PDP. Our findings suggest that enhanced Wnt signaling contributes to the development of pachydermia by enhancing dermal fibroblast functions. (Am J Pathol 2010, 176:721–732; DOI: 10.2353/ajpath.2010.090454)

Pachydermoperiostosis (PDP), a form of primary hypertrophic osteoarthropathy, is a rare disease^{1–3} diag-

nosed by the presence of a triad of pachydermia (skin thickening), digital clubbing, and periostosis of long bones. Typically, insidious development of thickening of the fingers and toes, clubbing of the terminal phalanges, enlargement of the hands and feet, hyperhidrosis, increased sebaceous secretion, and velvet coloration of the skin occur mostly in men during adolescence.⁴ Radiographic signs of bilateral and symmetrical periostosis are frequently observed as a marked irregular periosteal ossification of the tibiae and fibulae.³ Touraine et al⁵ recognized PDP with three clinical presentations or forms: a “complete form” presenting the full-blown phenotype; an “incomplete form” characterized by the phenotype without pachydermia; and a “fruste form” with pachydermia and minimal or absent skeletal changes.

Recently, the incomplete form of PDP, primary osteoarthropathy without pachydermia, was mapped to chromosome 4q33-q34, and gene mutations in *HPGD*, encoding 15-hydroxyprostaglandin dehydrogenase, the main enzyme of prostaglandin (PG) degradation, were identified.⁶ Therefore, it has been suggested that the digital clubbing and bone changes are due to elevated PGE₂. However, the pathomechanism underlying pachydermia of PDP remains unknown.

Since the major manifestations of complete PDP occur in both skin and bone, the etiology could be related to the dysregulation of bone morphogenetic proteins (BMP), transforming growth factor (TGF)- β , and/or wingless (Wnt) pathways.^{7–9} The Wnt signaling consists of canonical and non-canonical pathways. The canonical pathway involves cytosolic β -catenin stabilization, nuclear translocation and gene regulation, and the non-canonical pathways activate rho, rac, JNK, and protein kinase C.^{10,11} These signaling pathways are mediated by Wnt protein, which binds to a frizzled Wnt receptor. Wnt signaling is modulated by several different families of

Supported in part by grants from the Ministry of Education, Culture, Sports, Science and Technology and the Ministry of Health, Labour and Welfare of Japan.

K.K. and J.S. contributed equally to this work.

Accepted for publication October 20, 2009.

Address reprint requests to Dr. Kenji Kabashima, Department of Dermatology, Kyoto University Graduate School of Medicine, 54 Shogoin Kawaracho, Sakyo-ku, Kyoto 606-8507, Japan. E-mail: kaba@kuhp.kyoto-u.ac.jp.

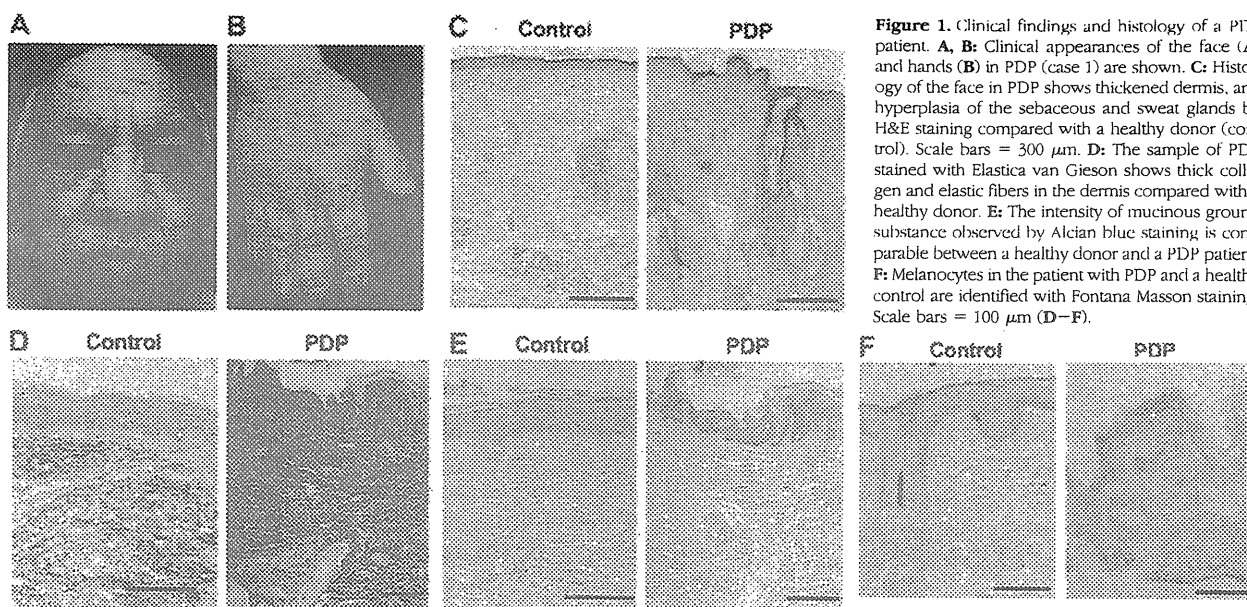


Figure 1. Clinical findings and histology of a PDP patient. **A, B:** Clinical appearances of the face (**A**) and hands (**B**) in PDP (case 1) are shown. **C:** Histology of the face in PDP shows thickened dermis, and hyperplasia of the sebaceous and sweat glands by H&E staining compared with a healthy donor (control). Scale bars = 300 μ m. **D:** The sample of PDP stained with Elastica van Gieson shows thick collagen and elastic fibers in the dermis compared with a healthy donor. **E:** The intensity of mucinous ground substance observed by Alcian blue staining is comparable between a healthy donor and a PDP patient. **F:** Melanocytes in the patient with PDP and a healthy control are identified with Fontana Masson staining. Scale bars = 100 μ m (**D-F**).

secreted down-regulators. Among them, Dickkopf (DKK) is a family of cysteine-rich proteins comprising at least four different forms (DKK1, DKK2, DKK3, and DKK4), which are coordinately expressed in mesodermal lineages. The best studied of these is DKK1, which blocks the canonical Wnt signaling by inducing endocytosis of lipoprotein receptor-related protein 5/6 (LRP5/6) complex¹² without affecting the frizzled Wnt receptor.¹³ DKK1 induces the formation of ectopic heads in *Xenopus laevis* in the presence of BMP inhibitors¹⁴ and modulates apoptosis during vertebrate limb development.¹⁵ High mRNA levels of *DKK1* in human dermal fibroblasts of the palms and soles inhibit the function and proliferation of melanocytes via the suppression of β -catenin and microphthalmia-associated transcription factor.^{16,17} In parallel, DKK1 transgenic mice under the control of keratin 14 have no pigmentation on the trunk because of the absence of melanocytes in the inner-follicular epidermis, as well as the lack of hair follicle development.¹⁸ These findings suggest that DKK1 is deeply involved in the formation and differentiation of the skin.

Here we investigated two complete cases of PDP using dermal fibroblasts to address the pathogenetic mechanisms. DNA microarray analysis revealed that the proliferation of primary fibroblasts of PDP was increased with decreased expression of *DKK1* mRNA in cultured fibroblasts. Consistent with this finding, immunohistochemistry indicated decreased expression of DKK1 in fibroblasts and enhanced expression of β -catenin in the skin of patients with PDP suggesting that Wnt signaling is enhanced in PDP. The intradermal injection of *DKK1* synthetic small interfering RNA (siRNA) increased the ear thickness of mice as seen in PDP. These results suggest that enhanced Wnt signaling contributes to the development of pachydermia.

Materials and Methods

Patients

Case 1

A 50-year-old male was referred to our clinic. The skin on his head and face was thick and oily with a dark velvet color. Naso-labial folds and transverse furrowing of the forehead were prominent (Figure 1A). The hands were enlarged with marked clubbing of the second and fifth digits, as compared with those of an age- and sex-matched healthy donor (Figure 1B). These symptoms developed when he was 18 years old. X-ray examination of the long bones showed major periostosis with cortical thickening and widening of the shafts (data not shown). Histology of the skin showed thickened dermis, and sebaceous and sweat gland enlargement, as compared with that of a healthy control (Figure 1C). Elastica van Gieson staining showed thick and interwoven collagen bundles in some areas of the dermis and also thick and partially fragmented elastic fibers in PDP (Figure 1D). The intensity of mucinous ground substance observed by Alcian blue staining was comparable between a healthy control and a PDP patient (Figure 1E). On the other hand, Fontana Masson staining revealed that the number of melanocytes and the intensity of the staining in the patient with PDP was higher than that in a healthy control (Figure 1F). Neither hepatosplenomegaly nor internal malignancy was found on physical examination or computed tomography scans. Biochemical tests showed normal levels of thyroid-stimulating hormone and growth hormone, which likely rules out thyroid acropathy and acromegaly. Family history was non-contributory. Based on these clinical manifestations and histological findings, the patient was diagnosed as the complete form of PDP.

Case 2

The patient was a 38-year-old male with clinical findings similar to case 1, including pachydermia, digital clubbing, and periostosis. He had no signs or symptoms of hepatosplenomegaly, pulmonary diseases, tumoral syndrome, thyroid acropathy, or acromegaly (data not shown) as reported previously.¹⁹

Cell Preparation, Culture, and Reagents

Skin biopsies of the right temple (case 1) and scalp (case 2) were performed for histology and primary culture of fibroblasts. Control donors were matched for age, sex, and biopsy site, and the samples were processed in parallel. Institutional approval and informed consent were obtained from all subjects. The biopsy samples were immersed in Dulbecco's Modified Eagle Medium (Sigma, St. Louis, MO) containing 10% heat-inactivated fetal calf serum (Invitrogen, Carlsbad, CA), 5×10^{-5} mol/L 2-mercaptoethanol, 2 mmol/L L-glutamine, 25 mmol/L HEPES (Cellgro, Herndon, VA), 1 mmol/L nonessential amino acids, 1 mmol/L sodium pyruvate, 100 units/ml penicillin, and 100 μ g/ml streptomycin, with 5% CO₂ at 37°C. The fibroblasts were allowed to adhere to the surface of 100-mm plastic tissue culture dishes (Nunc, Roskilde, Denmark). To evaluate the number of fibroblasts, 2×10^5 third-passage fibroblasts were seeded in 1 ml of medium in 24-well dishes and resuspended with trypsin/EDTA 1 week later. The numbers of fibroblasts were evaluated 7 and 14 days after seeding by flow cytometry using FACSCanto (BD Biosciences, San Diego, CA) with standard beads Flow Count (Beckman Coulter, Fullerton, CA) as per the manufacturer's instructions. The actin bundle formation of cultured fibroblasts from a healthy individual and an individual with PDP were examined by staining with alexa 488-labeled phalloidin antibody (Invitrogen) 5 days after the fourth passage.

For treatment with DKK1, fibroblasts were harvested 5 days after a comparable number of passages and cultured again at 1×10^6 cells in one ml of medium with or without recombinant human DKK1 (R&D Systems Inc., Minneapolis, MN) for another 2 days. For treatment with PGE₂, fibroblasts were harvested 5 days after a comparable number of passages and cultured again at 1×10^5 cells in two ml of medium with or without PGE₂ (Sigma) in the presence of indomethacin (10 μ mol/L; Cayman Chemical Co., Ann Arbor, MI) for another 4 days.

Flow Cytometry and Histology

Flow cytometric analysis was performed with doublet discrimination on the FACSCanto²⁰ and FlowJo software (TreeStar, San Carlos, CA).²¹ Human fibroblasts were treated with cytofix/cytoperm buffer according to the manufacturer's protocol (BD Biosciences). For cell cycle analysis, fibroblasts were incubated with 7-amino actinomycin D (7-AAD) (BD Biosciences) for 20 minutes at 4°C. After staining with 7-AAD, the DNA contents were analyzed by flow cytometry. For β -catenin staining, fibro-

blasts were stained with phycoerythrin-labeled β -catenin antibody (H-102, Santa Cruz Biotechnology Inc., Santa Cruz, CA), and mean fluorescence intensity was evaluated by flow cytometry.

For histology, the biopsy samples and the ears of mice were fixed in 10% formaldehyde. Sections of 5- μ m thickness were prepared and stained with H&E, Elastica van Gieson, or Alcian blue. Immunohistochemical staining on paraffin-embedded sections was performed using a Vectastain ABC kit (Vector Laboratories, Burlingame, CA).²⁰ Antibodies used were rabbit anti-human polyclonal DKK1 (ab61034, Abcam, Cambridge, UK), mouse monoclonal anti-human β -catenin IgG1 (610153, BD Biosciences, San Diego, CA), and rabbit anti-human polyclonal proliferating cellular nuclear antigen antibodies (SC-7907, Santa Cruz Biotechnology Inc., Santa Cruz, CA). The control antibodies used were rabbit non-immune serum or mouse IgG1 (X0931, Dako, Glostrup, Denmark). The immunoreactivity was visualized by Fast Red or diaminobenzidine (Sigma), and the sections were then counterstained with hematoxylin. Images were acquired on a 600CL-CU cooled charge-coupled device video camera (Pixera, Los Gatos, CA) and processed with InStudio 1.0.0 (Pixera).

Western Blot Analysis

For Western blotting studies, fibroblasts were isolated from a healthy donor. Cytoplasm- and nuclear- proteins were extracted by NucBuster Protein Extraction Kit (Novagen, Darmstadt, Germany). Twenty μ g protein samples were electrophoresed by 8% SDS-polyacrylamide gel electrophoresis and electroblotted onto polyvinylidene difluoride membranes for 2 hours at 180 mA. After blocking with 5% skim milk solution, the membranes were incubated with rabbit anti-human β -catenin (SC-7199; 1:1000, Santa Cruz Biotechnology Inc.) polyclonal antibodies or rabbit anti-human glyceraldehyde-3-phosphate dehydrogenase (SC-25778; 1:1000, Santa Cruz Biotechnology Inc.) antibody and detected with horseradish peroxidase-conjugated goat anti-rabbit IgG (Bio-Rad, Hercules, CA). Immunoblots were visualized using the ECL Plus Western Blotting Detection Reagents (GE Health care, Buckinghamshire, UK) according to the manufacturer's protocol. Bands were quantified by densitometry with the help of a CS Analyzer ver. 2.0 (ATTO, Tokyo, Japan).

Quantitative Reverse Transcription-PCR and Microarray Procedures

Total RNA was extracted from three-passage fibroblasts (case 1 and the control) cultured for 2 days with the RNeasy Mini Kit (QIAGEN, Valencia, CA). cDNA was reverse transcribed from total RNA samples using the TaqMan Reverse Transcription (RT) reagents (Applied Biosystems, Foster City, CA). Human *DKK1* (Assay ID: Hs00183740) mRNA expression was quantified using TaqMan Gene Expression Assay (Applied Biosystems) with the ABI PRISM 7700 sequence detection system (Applied Biosystems). As an endogenous reference for these RT-PCR quantification studies, human *GAPDH* con-

Table 1. PCR and Sequencing Primers

PCR Primer	Sequence	Tm	Binding site
hDKK1-Exon1, 2			
Forward	5'-CGTCTGCTATAACGCTCGCTGGTAG-3'	77	Promoter
Reverse	5'-AATTCATAGACGCTCAAAGGCTGGA-3'	73	Intron2
hDKK1-Exon3, 4			
Forward	5'-ACTTGCCCCCTACCACAGTTG-3'	70	Intron2
Reverse	5'-GTTCCCTGCCAATCACCAAGT-3'	68	3'UTR
hTCF-4-Exon1			
Forward	5'-TGGCTTTTCTTCCTCCTTCA-3'	66	5'UTR
Reverse	5'-AGAAAAAGAATCGGCGAGGT-3'	66	Intron1
hTCF-4-6			
Forward	5'-GCGATTTCTGGCAGGTAGTC-3'	70	Intron7
Reverse	5'-TAGCGATCCAGGAAGATGCT-3'	68	Intron10
hTCF-4-9			
Forward	5'-TTAGTAGGGGTGGGGGAAG-3'	70	Intron13
Reverse	5'-TTGGTAGAATCATGAGGTCTTCTC-3'	71	3'UTR
hHPGD Exon1			
Forward	5'-GCTGGCTTGACAGTTTCCTC-3'	70	5'UTR
Reverse	5'-CAGCCTCAGCTTCAGCAAAT-3'	68	Intron1
hHPGD Exon2			
Forward	5'-TTGCTGAAGCTGAGGCTGT-3'	68	Intron1
Reverse	5'-TCTTGCCCTTCTTTTCGGTTT-3'	64	Intron2
hHPGD Exon3			
Forward	5'-TCCACAAACCACACATTGAGA-3'	67	Intron2
Reverse	5'-CCAGCTTCTGTAACTTCCTTT-3'	70	Intron3
hHPGD Exon4			
Forward	5'-TAGGCAAACCCAAAGAATCC-3'	66	Intron3
Reverse	5'-CACATGGGAGCAGAGACATC-3'	70	Intron4
hHPGD Exon5			
Forward	5'-CCTGGGGAGGCAGAAAAA-3'	67	Intron4
Reverse	5'-TTTATTTGGTTCTTTATGTGATCTGA-3'	67	Intron5
hHPGD Exon6			
Forward	5'-TGCAGAGTTCAGTAGATAAGAGAAGC-3'	73	Intron5
Reverse	5'-TGCTTGGAATTTAGGCAGAGA-3'	67	Intron6
hHPGD Exon7			
Forward	5'-TTGGAAGTAGCAATAGTTTAATGA-3'	68	Intron6
Reverse	5'-TCACCAAGTGCATGAAGGAA-3'	66	3'UTR
Sequencing Primer	Sequence		Binding site
hDKK1-Exon1, 2			
Forward	5'-CGTCTGCTATAACGCTCGCTGGTAG-3'		Promoter
Reverse	5'-AATTCATAGACGCTCAAAGGCTGGA-3'		Intron2
hDKK1-Exon1-S2			
Forward	5'-CCACCTTGAACCTCGGTCTC-3'		Exon1
hDKK1-Exon2-S1			
Forward	5'-AGAACGTGCTGAATGTGTGC-3'		Intron1
hDKK1-Exon3, 4			
Forward	5'-ACTTGCCCCCTACCACAGTTG-3'		Intron2
Reverse	5'-GTTCCCTGCCAATCACCAAGT-3'		3'UTR
hDKK1-Exon3-S1			
Forward	5'-CCTTGATGGGTATTCCAGA-3'		Exon3
hDKK1-Exon4-S1			
Forward	5'-TCATCAGACTGTGCCTCAGG-3'		Exon4
hDKK1-Exon4-S2			
Forward	5'-AAGGTGCTGCACTGCCTATT-3'		3'UTR
hTCF-4-Exon1			
Forward	5'-TGGCTTTTCTTCCTCCTTCA-3'		5'UTR
Reverse	5'-AGAAAAAGAATCGGCGAGGT-3'		Intron1
hTCF-4-Exon9			
Forward	5'-GCTTGGGGTTATGAGACAA-3'		Intron8
Reverse	5'-AGACATTCTGCCACCTGACC-3'		Intron9
hTCF-4-Exon10			
Forward	5'-CCTTGGCGTAATGTGTGATG-3'		Intron9
Reverse	5'-TAGCGATCCAGGAAGATGCT-3'		Intron10
hTCF-4-Exon14			
Forward	5'-ACATCCCTTAGGTGACCTCA-3'		Intron13
Reverse	5'-GGGGCAAATTAAGAAAAGTG-3'		3'UTR

(table continues)

Table 1. *Continued*

Sequencing Primer	Sequence	Binding site
hHPGD Exon1		
Forward	5'-GCTGGCTTGACAGTTTCCTC-3'	5'UTR
Reverse	5'-CAGCCTCAGCTTCAGCAAAT-3'	Intron1
hHPGD Exon2		
Forward	5'-TTGCTGAAGCTGAGGCTGT-3'	Intron1
Reverse	5'-TCTTGCCCTTCTTTCGGTTT-3'	Intron2
hHPGD Exon3		
Forward	5'-TCCACAAACCACACATTGAGA-3'	Intron2
Reverse	5'-CCAGCTTCTGTAACTTCCCTTT-3'	Intron3
hHPGD Exon4		
Forward	5'-TAGGCAAACCCAAAGAATCC-3'	Intron3
Reverse	5'-CACATGGGAGCAGACATC-3'	intron4
hHPGD Exon5		
Forward	5'-CCTGGGGAGGCAGAAAAA-3'	Intron4
Reverse	5'-TTTATTTGGTTCTTTATGTGATCTGA-3'	Intron5
hHPGD Exon6		
Forward	5'-TGCAAGTTCAGTAGATAAGAGAAGC-3'	Intron5
Reverse	5'-TGCTTGAATTTAGGCAGAGA-3'	Intron6
hHPGD Exon7		
Forward	5'-TTGGAAGTAGCAATAGTTTAATGA-3'	Intron6
Reverse	5'-TCACCAAGTGCATGAAGAA-3'	3'UTR

The exons of DKK1, TCF7L2 (TCF-4), and HPGD genes were amplified via PCR in a thermal cycler using the forward and reverse primer pairs indicated in the upper list. Direct sequencing was performed with the BigDye Terminator v3.1 Cycle Sequencing Kit and sequencing primers indicated in the lower list. Binding sites of primers are also indicated.

control reagents (Assay ID: Hs99999905) (Applied Biosystems) were used. The relative expression was calculated using the $\Delta\Delta$ Ct method.²²

For DNA microarray analysis, total RNAs were extracted from fibroblasts with the RNeasy Mini Kit (QIAGEN). For transcriptomic profiling, we used an oligonucleotide-based DNA microarray, AceGene (HumanOligoChip30K, DNA Chip Research, Yokohama, Japan). Images were analyzed with DNASIS Array (Hitachi Software Engineering, Tokyo, Japan), according to the manufacturer's instructions. Mean

and SD of background levels were calculated, and genes with intensities less than mean plus 2SD of background levels were excluded from further analysis. The Cy5/Cy3 ratios of all spots on the DNA microarray were normalized by the method of global normalization.

Genetic Analysis for DKK1, TCF, and HPGD

Three healthy controls and two PDP patients (cases 1 and 2) were enrolled and followed up according to local

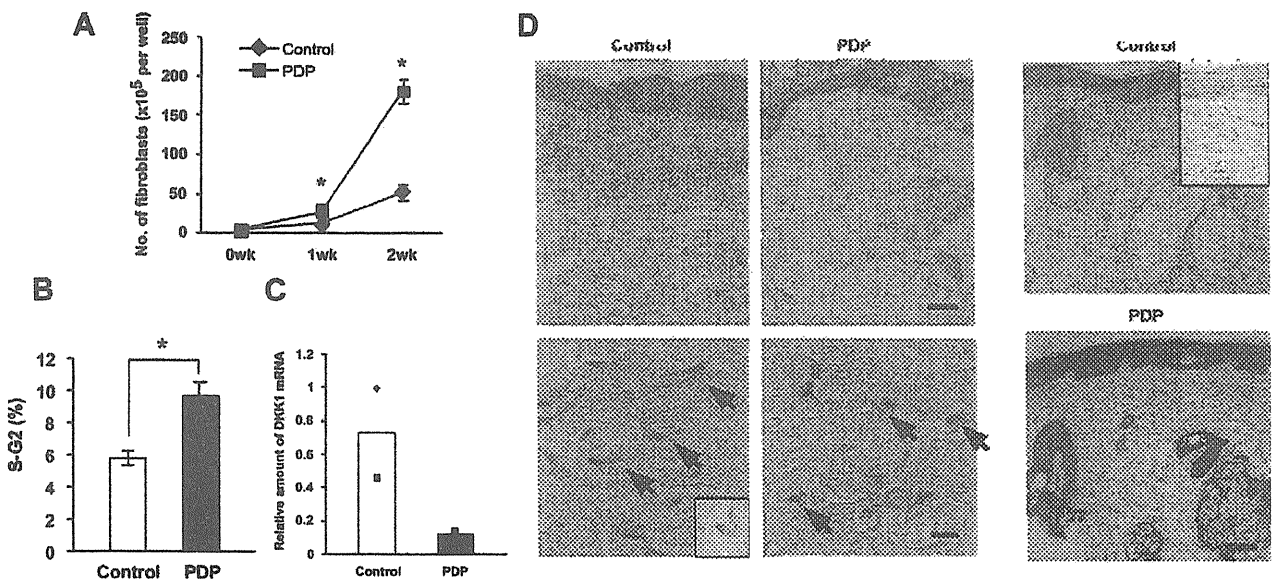


Figure 2. Characteristics of dermal fibroblasts and histology of the skin in PDP. **A:** Fibroblasts from a healthy individual (control) and an individual with PDP (case 1) (PDP) were incubated and the numbers of fibroblasts examined. **B:** The percentages of fibroblasts in S-G2 phase are shown. **C:** The levels of *DKK1* mRNA in fibroblasts from two controls and two PDPs were normalized against GAPDH, and the level of one of the control *DKK1* mRNAs is regarded as one. Filled symbols indicate two independent individuals and columns represent the average. **D** and **E:** Skin sections were stained with anti-human DKK1 (**D**) and β -catenin (**E**) antibodies. **Arrows** show the perinuclear area of fibroblasts (**D**). Scale bars: upper panels (150 μ m), and lower panels, 10 μ m (**D**), and 100 μ m (**E**). We include that the controls incorporating non-immune serum (**D**) or mouse IgG1 (**E**) as insets show no specific reactivity. The student's *t*-test was performed ($*P < 0.05$) (**A**, **B**).

Table 2. DNA Microarray Analysis

Gene names	Accession ID	Expression levels		Difference	Fold difference
		Control	PDP		
<i>BMP2</i>	NM_001200_1	5.72	5.87	0.16	—
<i>BMP3</i>	M22491_1	ND	ND	NA	—
<i>BMP4</i>	NM_001202_1	7.20	7.46	0.26	—
<i>BMP5</i>	NM_021073_1	4.61	4.30	-0.30	—
<i>BMP6</i>	NM_001718_1	4.34	4.96	0.61	—
<i>BMP7</i>	NM_001719_1	ND	ND	NA	—
<i>BMP8B</i>	NM_001720_1	5.47	5.65	0.18	—
<i>BMP10</i>	NM_014482_1	ND	ND	NA	—
<i>BMP15</i>	NM_005448_1	ND	ND	NA	—
<i>TGFB1</i>	NM_000660_1	8.87	7.91	-0.97	—
<i>TGFB2</i>	NM_003238_1	4.34	5.05	0.72	—
<i>TGFBR1</i>	NM_004612_1	ND	ND	NA	—
<i>TGFBR2</i>	NM_003242_1	ND	ND	NA	—
<i>TGFBR3</i>	NM_003243_1	4.34	4.51	0.17	—
<i>WNT1</i>	NM_005430_1	6.66	5.45	-1.21	0.4
<i>WNT2</i>	ENSG00000105989	ND	ND	NA	—
<i>WNT2B</i>	NM_024494_1	6.36	6.95	0.60	—
<i>WNT4</i>	AY009398_1	4.33	4.35	0.03	—
<i>WNT5A</i>	NM_003392_1	5.36	5.85	0.50	—
<i>WNT6</i>	BC004329_1	5.13	4.99	-0.14	—
<i>WNT7A</i>	NM_004625_1	ND	ND	NA	—
<i>WNT8B</i>	NM_003393_1	7.27	6.88	-0.39	—
<i>WNT9A</i>	AB060283_1	7.36	6.92	-0.44	—
<i>WNT9B</i>	AF028703_1	5.69	4.47	-1.22	0.4
<i>WNT10A</i>	NM_025216_1	4.40	5.40	1.00	—
<i>WNT10B</i>	NM_003394_1	5.73	4.48	-1.25	0.4
<i>WNT11</i>	NM_004626_1	6.46	5.85	-0.61	—
<i>WNT16</i>	NM_016087_1	7.63	6.80	-0.83	—
<i>FZD1</i>	NM_003505_1	7.19	6.91	-0.28	—
<i>FZD2</i>	AB017364_1	7.05	7.01	-0.03	—
<i>FZD3</i>	AJ272427_1	7.51	6.85	-0.67	—
<i>FZD3</i>	NM_017412_1	ND	ND	NA	—
<i>FZD4</i>	NM_012193_1	6.09	6.49	0.41	—
<i>FZD5</i>	NM_003468_1	5.02	5.44	0.42	—
<i>FZD6</i>	NM_003506_1	5.95	6.37	0.42	—
<i>FZD7</i>	NM_003507_1	9.32	9.40	0.08	—
<i>FZD8</i>	AB043703_1	ND	ND	NA	—
<i>DKK1</i>	NM_012242_1	11.61	8.46	-3.15	0.1
<i>DKK2</i>	NM_014421_1	6.53	6.93	0.40	—
<i>DKK3</i>	NM_015881_1	9.24	9.15	-0.08	—
<i>KREMEN1</i>	AB059618_1	ND	ND	NA	—
<i>KREMEN2</i>	NM_024507_1	5.20	4.33	NA	—
<i>COL1A1</i>	K03179_1	7.57	7.90	0.34	—
<i>COL1A2</i>	NM_000089_1	13.54	13.98	0.44	—
<i>COL2A1</i>	NM_033150_1	9.46	10.09	0.63	—
<i>COL3A1</i>	NM_000090_1	10.26	11.43	1.17	2.3
<i>COL4A1</i>	NM_001845_1	8.66	7.83	-0.83	—
<i>COL4A2</i>	X05562_1	7.17	6.83	-0.34	—
<i>COL4A3</i>	U02519_1	4.54	5.04	0.49	—
<i>COL4A4</i>	NM_000092_1	4.73	4.30	-0.43	—
<i>COL4A5</i>	NM_000495_1	4.23	5.72	1.50	2.8
<i>COL4A6</i>	D63562_1	8.41	8.68	0.28	—
<i>COL5A1</i>	BC008760_1	10.35	10.25	-0.09	—
<i>COL5A3</i>	NM_015719_1	5.57	6.20	0.62	—
<i>COL6A2</i>	AY029208_1	10.90	10.62	-0.29	—
<i>COL6A3</i>	NM_004369_1	6.64	5.37	-1.27	0.4
<i>COL8A1</i>	NM_001850_1	10.47	11.09	0.61	—
<i>COL8A2</i>	M60832_1	5.43	5.55	0.11	—
<i>COL9A1</i>	NM_001851_1	6.97	6.84	-0.13	—
<i>COL9A2</i>	NM_001852_1	4.15	6.13	1.98	4
<i>COL9A3</i>	NM_001853_1	4.73	5.17	0.44	—
<i>COL10A1</i>	NM_000493_1	4.10	6.90	2.80	7
<i>COL11A1</i>	NM_001854_1	6.45	9.28	2.84	7
<i>COL11A2</i>	JO4974_1	ND	ND	NA	—
<i>COL12A1</i>	NM_004370_1	4.98	6.26	1.27	2.5

(table continues)

Table 2. *Continued*

Gene names	Accession ID	Expression levels		Difference	Fold difference
		Control	PDP		
<i>COL14A1</i>	Y11711_1	4.21	5.81	1.60	3
<i>COL15A1</i>	NM_001855_1	ND	ND	NA	—
<i>COL17A1</i>	NM_000494_1	4.32	6.33	2.01	4
<i>COL18A1</i>	NM_030582_1	5.73	6.03	0.30	—
<i>COL19A1</i>	NM_001858_1	ND	ND	NA	—
<i>FN1</i>	X07717_1	7.10	6.69	−0.41	—
<i>FN5</i>	NM_020179_1	6.41	6.71	0.30	—
<i>ELN</i>	NM_000501_1	7.60	7.33	−0.26	—

The upper list of genes related to BMP, TGF- β , and Wnt signaling. The lower list of genes is related to collagens, fibronectins, and elastin. The mRNA expression levels of a healthy donor (control) and the individual with PDP (PDP) are normalized by LOWESS normalization, and indicated by log2. The values in Difference indicate mRNA expression levels of the individual with PDP—those of the healthy individual. The values under 'Fold Difference' indicate mRNA expression levels of the individual with PDP/those of the healthy individual, ie, Log2(Difference). The symbol "—" in the Fold Difference indicates non-significant difference between the healthy donor and the individual with PDP. ND, not determined. NA, not applicable.

ethical guidelines. Genomic DNA was isolated from primary fibroblasts or peripheral blood leukocytes using proteinase K and the PCI (phenol/chloroform/isoamyl alcohol) extraction procedure. The *DKK1* (GenBank: NM012242), *TCF7L2* (*TCF-4*) (GenBank: NM030756), and *HPGD* (NM000860) genes were amplified via PCR in a thermal cycler (Eppendorf, Hamburg, Germany) using forward and reverse primer pairs (Table 1).

Amplified products were purified with the QIAquick Gel Extraction Kit (QIAGEN, Valencia, CA) or Wizard SV Gel and PCR Clean-Up System (Promega, Madison, WI) after 1.5% agarose electrophoresis. Direct sequencing was performed with the BigDye Terminator v3.1 Cycle Sequencing Kit (Applied Biosystems, Foster City, CA) and sequencing primers (Table 1) using capillary electrophoresis (ABI Prism 3130xl Genetic Analyzer; Applied Biosystems), and analyzed with ABI Prism DNA Sequencing Analysis software ver. 5.1 (Applied Biosystems) as previously described.²³

Application of Mouse *DKK1* siRNA

Mouse *DKK1* siRNA (5'-GAA CCA CAC UGA CUU CAA ATT-3') was purchased from Nippon EGT (Toyama, Japan). siRNA duplexes were generated by mixing sense and antisense single-stranded RNA oligomers equally in an annealing buffer (NIPPON EGT).²⁴ Negative control siRNA (AM4611) was purchased from Ambion (Austin, TX). To impregnate mouse *DKK1* siRNA into cationized gelatin microspheres,²⁵ 10 μ l of PBS solution (pH 7.4) containing 10 μ g of mouse *DKK1* siRNA was dropped onto 1 mg of the freeze-dried cationized gelatin microspheres, kept overnight at 4°C, and added to 190 μ l of PBS. Ten μ l of this siRNA solution was injected intradermally into the center of the ears of 8-week-old C57BL/6j female mice (obtained from SLC, Shizuoka, Japan) using a 30-gauge needle four times every 7 days. The same amount of cationized gelatin-conjugated nonsense siRNA was applied as a negative control. The ear thickness was measured before each injection and one week after the last injection using dial-thickness gauge (PG-01, TECLOCK, Okaya, Japan). The injected area was sampled for histology and RT-PCR analysis using 6-mm punch biopsy. Mice were maintained on a 12-hour light/

dark cycle under specific pathogen-free conditions. Protocols were approved by the Institutional Animal Care and Use Committee of the University of Occupational and Environmental Health.

Statistical Analysis

Data were analyzed using an unpaired two-tailed *t*-test. A *P* value of less than 0.05 was considered to be significant.

Results

Increased S-G2 Phase in Fibroblasts of PDP

Case 1 had a typical complete form of PDP (Figure 1, A and B) characterized by the triad of pachydermia, digital clubbing, and periostosis.^{1–3} The histology of the skin showed thickened dermis with dense and packed collagen and elastic fibers (Figure 1, C–E), suggesting that the function of fibroblasts was enhanced in PDP. To test the proliferative activity of fibroblasts, we cultured primary fibroblasts from case 1 and a matched control, and monitored their number. As reported previously,²⁶ the number of PDP fibroblasts was significantly higher than that of control fibroblasts (Figure 2A). Similar results were obtained in another typical patient with PDP, case 2 (data not shown). To clarify whether it was due to enhanced cell survival or proliferation, we stained the nuclear contents of fibroblasts with 7-AAD for cell cycle analysis. The ratio of PDP fibroblasts in the cell cycle (S-G2 phase) was higher than that of control fibroblasts (Figure 2B), suggesting that the proliferation of fibroblasts was enhanced in PDP.

Decreased *DKK1* Expression in PDP Fibroblasts and Skin

The above results together with the clinical phenotypes involving the skin and bone suggested the possibility that the pathogenesis of PDP is related to dysregulation of BMP, Wnt, and/or TGF- β pathways in mesenchymal cells. To efficiently compare the expression profiles of these genes between PDP fibroblasts (case 1) and matched controls,

DNA microarray analysis was performed and the complete array data were deposited in a MIAME-compliant microarray database (GSE17947). Among all genes analyzed, 2573 genes were elevated and 2346 genes were decreased more than twofold in PDP patients compared with a healthy control. The analysis revealed that the mRNA levels of *BMP* and *TGF- β* families were comparable between these two groups (Table 2). On the other hand, *WNT1*, *WNT10B*, and *DKK1* mRNAs were decreased in the patient's fibroblasts (Table 2). In particular, *DKK1* mRNA was markedly decreased. Other molecules, such as levels of *LRP5/6*, *Kremen1*, and *Kremen2* mRNA were similar between these two groups (Table 2). Moreover, the mRNA levels for collagen families, such as *COL4A5*, *COL9A2*, *COL10A1*, *COL11A1*, *COL12A1*, *COL14A1*, and *COL17A1*, were elevated, but those for *fibronectin* and *elastin* (*ELN*) families were not (Table 2). These data suggest that the PDP fibroblasts showed enhanced production of several types of collagens in addition to cell proliferation, which might explain the pathogenesis of pachydermia in PDP.

We initially confirmed the decreased *DKK1* expression using quantitative RT-PCR. Fibroblasts were primarily cultured from two PDP patients (cases 1 and 2) and two matched healthy controls. *DKK1* mRNA levels in PDP fibroblasts were consistently lower than those in the control fibroblasts (Figure 2C). We then performed immunohistochemical analysis to evaluate the expression of *DKK1* protein in the PDP skin (case 1) and the control. In the normal skin, *DKK1* was detected diffusely in the dermis (Figure 2D, upper panels) and notably in the cytoplasm of fibroblasts (Figure 2D, lower panels). The intensity of this expression pattern was substantially decreased in the PDP patient (case 1) (Figure 2D, lower panels). This finding was confirmed with the other PDP patient (case 2) and another matched control (data not shown). We displayed that the controls incorporating non-immune serum (inset, Figure 2D) or mouse IgG1 (inset, Figure 2E) show no specific reactivity.

The decreased expression of *DKK1* in PDP suggested that Wnt signaling is enhanced in PDP. Immunohistochemical analysis revealed enhanced β -catenin expression in the PDP skin (case 1), especially around the sebaceous glands, the hair follicles, and the epidermis, and mildly in the dermis, as compared with the control (Figure 2E), supporting the augmented expression of Wnt signaling.

Suppression of Fibroblast Proliferation by *DKK1*

The above results indicated that Wnt signaling is enhanced in PDP through decreased *DKK1* expression. However, it was still unknown whether *DKK1* directly modulates the function of dermal fibroblasts. To solve this issue, we cultured dermal fibroblasts from a healthy control and the patient with PDP (case 1) in the presence or absence of human recombinant *DKK1*, and quantitated the DNA contents of fibroblasts by cell cycle analysis with 7-AAD. The ratio of fibroblasts in the cell cycle (S-G2 phase) was higher in the PDP patient than in the control (Figure 3, A and B). In addition, the ratio of fibroblasts with the cell cycle (S-G2 phase) was decreased by treat-

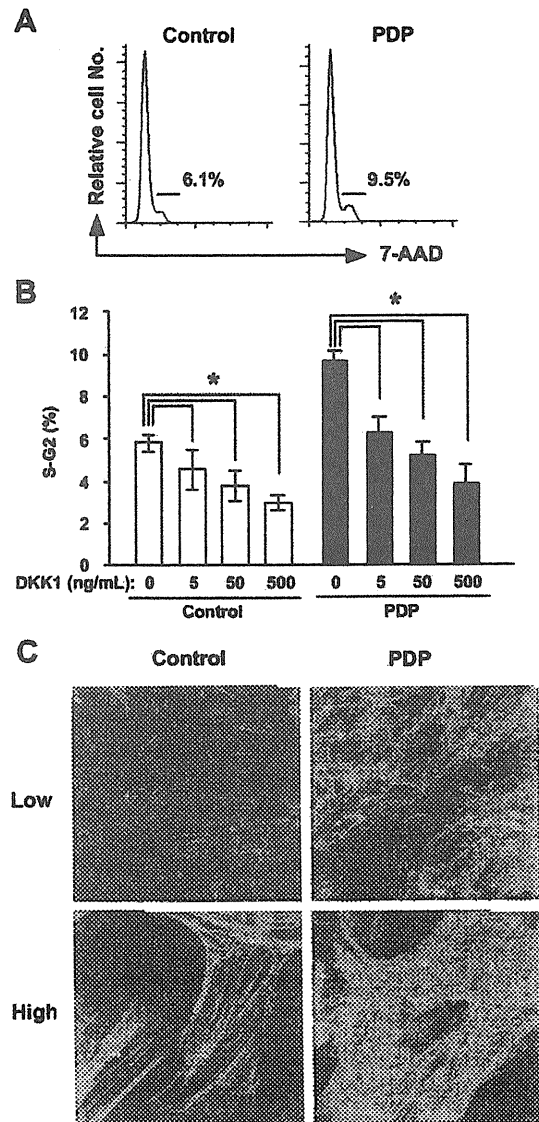


Figure 3. The effect of *DKK1* on fibroblast proliferation and actin bundle formation of fibroblasts. **A, B:** The fibroblasts from a healthy individual (control) and an individual with PDP (PDP) were incubated with or without recombinant human *DKK1* protein and the DNA contents of fibroblasts were evaluated with 7-AAD using flow cytometry. Representatives of FACS plots of fibroblasts from a healthy individual (control) and an individual with PDP (PDP) are shown (A). The percentages of fibroblasts in S-G2 phase in triplicated wells are expressed as the mean \pm SD ($n = 3$). The student's *t*-test was performed between the indicated groups and $*P < 0.05$. **C:** The actin bundle formation of cultured fibroblasts from a healthy individual (control) and an individual with PDP (PDP) were examined by staining with alexa 488-labeled phalloidin antibody 5 days after the fourth passage. Upper panels, low magnification ($\times 10$); lower panels, high magnification ($\times 40$).

ment with recombinant *DKK1* protein in a dose-dependent manner (Figure 3B), implicating the direct involvement of *DKK1* in fibroblast proliferation.

Enhanced Actin Bundle Formation of Fibroblasts in PDP

Wnt signaling is also known to induce cell motility and cytoskeletal rearrangement of NIH3T3, a fibroblast cell line.²⁷ Therefore, we examined the actin bundle formation

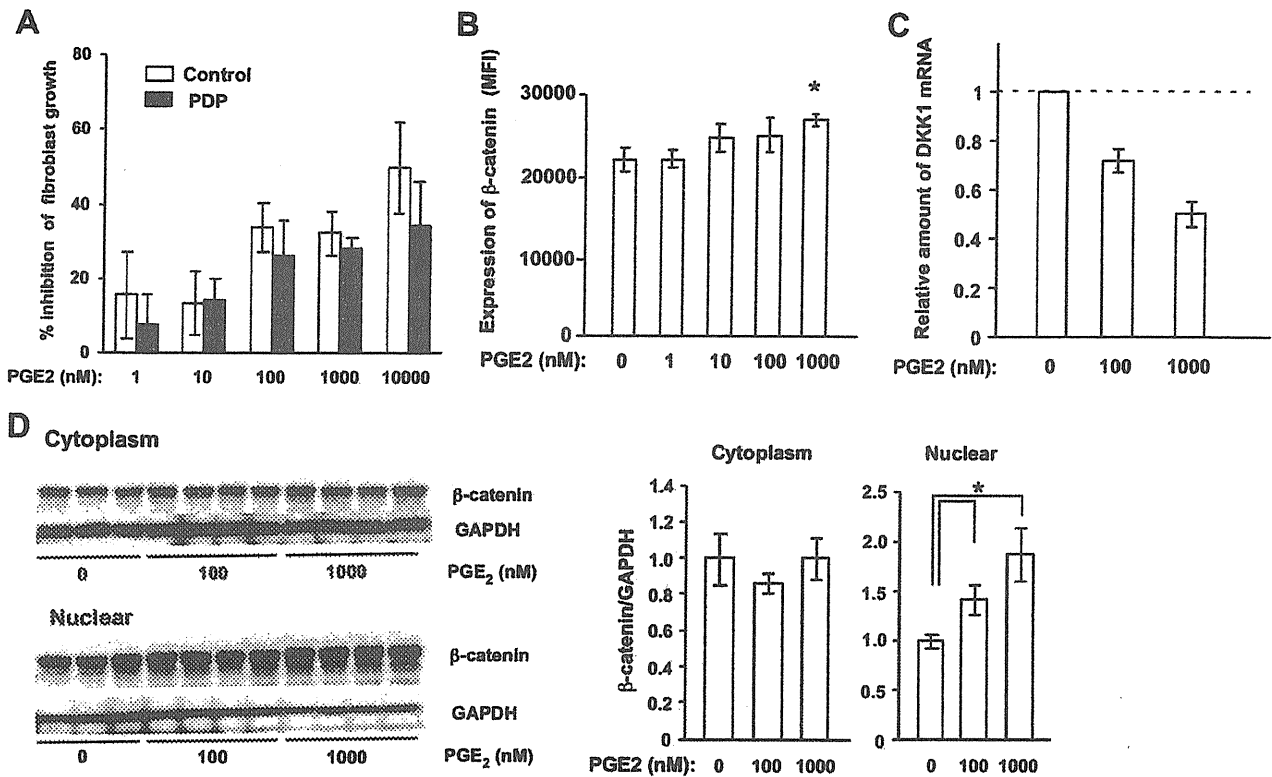


Figure 4. Effect of PGE₂ on fibroblasts. **A:** The % inhibition of the number of fibroblasts from a healthy donor and a PDP patient by the addition of PGE₂ was evaluated as (Number of fibroblasts without PGE₂ - Number of fibroblasts with PGE₂)/Number of fibroblasts without PGE₂ × 100. The growth inhibitory effect of PGE₂ is dose-dependent and comparable between these two groups. The values are expressed as the mean ± SD (*n* = 3) and are representative of two independent experiments. **B, C:** The effects of PGE₂ on β-catenin expression and *DKK1* mRNA levels in fibroblasts were evaluated. The mean fluorescent intensity (MFI) of β-catenin (**B**) and *DKK1* mRNA (**C**) in fibroblasts after exposure to PGE₂ is shown. The amount of *DKK1* mRNA relative to *GAPDH* mRNA without the addition of PGE₂ is regarded as one. The values are expressed as the mean ± SD (*n* = 3) and **P* < 0.05. **D:** Cytoplasm- (right panel) and nuclear- (left panel) protein samples from fibroblasts treated with or without 0, 100, and 1000 nmol/L PGE₂ for 4 days were used to determine the effect of PGE₂ on β-catenin expression. The values are expressed as the mean ± SD (*n* = 3 to 4) and **P* < 0.05.

of cultured fibroblasts with phalloidin staining 5 days after the fourth passage. Fluorescent microscopy showed that the actin bundle formation of PDP fibroblasts is promoted in PDP, as the bundles were thicker and denser than those of control fibroblasts (Figure 3C).

Effect of PGE₂ on Fibroblasts

It was recently reported that the incomplete form of PDP is induced by elevated PGE₂ due to a mutation in the *HPGD* gene.⁶ If this PGE₂ alteration also affects pachydermia, PGE₂ would be expected to enhance fibroblast function and proliferation. The addition of PGE₂ into the cultured medium of fibroblasts decreased the number of dermal fibroblasts from healthy donors in a dose-dependent manner as reported previously^{28,29} (Figure 4A). A similar effect was observed when PGE₂ was added to the culture medium of fibroblasts from the PDP patient (case 2). To examine whether PGE₂ affects Wnt signaling in fibroblasts, we measured the amount of β-catenin in fibroblasts after exposure to PGE₂ by flow cytometry, and found that β-catenin was significantly increased in fibroblasts by the addition of PGE₂ at a dose of 1000 nmol/L (Figure 4B). In addition, the mRNA expression level of *DKK1* was significantly decreased by the addition of PGE₂ at a dose of 100 and 1000 nmol/L (Figure 4C). Moreover, to determine the effect of

PGE₂ on β-catenin expression, cytoplasm- and nuclear-protein samples were prepared from fibroblasts treated with or without 0, 100, and 1000 nmol/L PGE₂ in the presence of 10 μmol/L indomethacin for 4 days. In the cytoplasm, β-catenin expression was unchanged irrespective of the addition of PGE₂. However, β-catenin expression in the nuclei was significantly increased by the treatment with 100 and 1000 nmol/L PGE₂ (Figure 4D). These results suggest that PGE₂ signaling increases nuclear β-catenin in fibroblasts.

Genetic Analysis for *DKK1*, *TCF-4*, and *HPGD* Genes

To address the cause of PDP, we initially analyzed the sequences of *HPGD*, and found no mutation including single nucleotide polymorphism that was different among three healthy donors and two PDP patients (data not shown). Rather, our current results suggest that the pathogenesis of the complete form of PDP may be attributable to enhanced Wnt signaling secondary to decreased *DKK1* expression. Moreover, it remains uncertain how *DKK1* expression is reduced in PDP. One possible mediator is *TCF7L2* (*TCF-4*), which binds to the *DKK1* promoter, thus enhancing activity of *DKK1*.³⁰